Synthesis and crystal structures of two nickel coordination polymers generated from asymmetric malate ligand

Yaqin Guo, Dongrong Xiao, Enbo Wang*, Ying Lu, Jian Lü, Xinxin Xu, Lin Xu

Department of Chemistry, Institute of Polyoxometalate Chemistry, Northeast Normal University, Changchun 130024, P.R. China

Abstract

Two nickel coordination polymers $[Ni(H_2O)(C_4H_4O_5)] \cdot H_2O$ **1** and $[Ni(H_2O)(mal)(phen)]$ **2**, have been hydrothermally synthesized and structurally characterized by single crystal X-ray diffraction. Crystal data for **1**: $C_4H_8O_7Ni$, monoclinic Cc, $a = 13.156(3)$ Å, $b = 7.5436(15)$ Å, $c = 9.6982(19)$ Å, $\beta = 130.96(3)°$, $Z = 4$. Crystal data for **2**: $C_{16}H_{14}N_2O_6Ni$, orthorhombic $Pna2_1$, $a = 9.6113(19)$ Å, $b = 19.691(4)$ Å, $c = 8.0944(16)$ Å, $Z = 4$. Compound **1** is constructed from $[Ni(H_2O)(C_4H_4O_5)]$ sheets pillared through β-carboxylate groups into a 3D framework, which exhibits a diamond-like network. Compound **2** exhibits a 3D supramolecular network. To our knowledge, compound **1** represents the first diamond-like topology in the system of metal–malate. Other characterizations by elemental analysis, IR and TG are also described. The magnetic behavior of compound **1** has been studied.

© 2005 Elsevier Inc. All rights reserved.

Keywords: Hydrothermally synthesized; Cavities; Crystal structures; Malate; Diamond-like; Magnetic

1. Introduction

Crystal engineering of metal-organic networks via self-assembly of metal ions and multifunctional ligands has attracted considerable research attention [1,2]. In particular, these metal-organic frameworks can be designed to create cavities or channel structures of various sizes and shapes, and they might find potential applications in many fields [3–5]. There are currently two main strategies used in designing such open frameworks, based on the use of either covalent bonds or weaker intermolecular interactions. Recently, numerous coordination complexes have been successfully designed and synthesized by utilizing saturated aliphatic carboxylate spacers, e.g. malonate, oxalate, glutarate, etc. owing to their conformational and coordination versatilities [6–9]. However, the system with malic acid as bridging ligand remains largely unexplored. Malic

acid, which is a hydroxycarboxylic acid and exists widely in biological media, is proposed as a cheap and "green" chemical reagent. Meanwhile, malate ligand is also an asymmetric spacer and can be assembled around metal centers in diverse arrangement, consequently resulting in multidimensional coordination polymers with intriguing structural topologies and pores. A small number of complexes have been isolated in the solid state and characterized by X-ray analyses [10,11]. The strong curiosity for unknown structures evokes us to explore the simple system of metal–malate ligand. Our previous investigation on self-assembly of Cu salt and malic acid under ambient condition produced a porous supramolecular coordination polymer $[Cu(mal)(bpy)] \cdot 3H_2O$ **L**, constructed from infinite spiral-shaped coordination polymeric chains via O–H⋯O hydrogen bonds and aromatic $\pi - \pi$ stacking interactions [12]. Here, we report two nickel–malate complexes prepared via hydrothermal reactions, formulated as $[Ni(H_2O)(C_4H_4O_5)] \cdot H_2O$ **1** and $[Ni(H_2O)(mal)(phen)]$ **2** (mal–malic acid, phen = 1,10-phenanthroline). Interestingly,

*Corresponding author. Fax: +86 431 5098787.

E-mail address: wangenbo@public.cc.jl.cn (E. Wang).

compound **1** exhibits a diamond-type network consisting of multidirectional 1D channels. Compound **2** exhibits a 3D supramolecular framework constructed from infinite spiral-shaped coordination polymeric chains. To the best of our knowledge, compound **1** is the first example of diamond-like framework in the system of metal–malate. The variable-temperature magnetic susceptibility of compound **1** was studied.

2. Experimental

2.1. Synthesis and characterization

Synthesis of $[Ni(H_2O)(C_4H_4O_5)] \cdot H_2O$, **1**. A mixture of $Ni(NO_3)_2 \cdot 6H_2O$ (0.5 mmol), malic acid (0.5 mmol) in 8 mL H_2O was stirred for 30 min, then the pH was adjusted to 4.5 with diluted NaOH solution, and transferred into a Parr Teflon-lined stainless steel Vessel (18 mL). The Vessel was sealed and heated to 160 °C for 5 d, followed by cooling at 10 °C h^{-1} to room temperature. Green block crystals of compound **1** were collected [yield: 82% based on Ni]. The effects of pH variation seemed so crucial for the quality and yield of crystals. The elemental analyses found: C, 21.01%; H, 3.45%; Ni, 25.69%; Calc. for $C_4H_8NiO_7$: C, 21.18%; H, 3.56%; Ni, 25.88%.

Compound **2** was prepared with the similar synthetic condition. A mixture of $Ni(NO_3)_2 \cdot 6H_2O$, malic acid and 1,10′-phen with the mole ratio of 1:1:1 was stirred for half an hour in 8 mL H_2O and the pH value was adjusted to 5.0 with diluted NaOH solution. Other experiment conditions are same as synthesis of compound **1** [yield: 42% based on Ni]. The elemental analyses found: C, 49.26%; H, 3.56%; N, 7.31%; Ni, 15.25%; Calc. for $C_{16}H_{14}N_2NiO_6$: C, 49.38%; H, 3.63%; N, 7.20%; Ni, 15.10%.

Elemental analyses (C, H and N) were performed on a Perkin–Elmer 2400 CHN Elemental Analyzer. Ni was determined by a Leaman inductively coupled plasma spectrometer. IR spectra were recorded in the range of 400–4000 cm^{-1} on an Alpha Centaurt FT/IR Spectrophotometer using KBr pellet. TG analyses were performed on a Perkin–Elmer TGA7 instrument in flowing N_2 with a heating rate of 10 °C min^{-1}. Variable-temperature magnetic susceptibility was measured at 10000 Oe from 2 to 300 K (SQUID, Quantum Design).

2.2. X-ray crystallography

Crystal data for compounds **1** and **2** were collected on a Rigaku R-AXIS RAPID IP diffractometer using graphite monochromatic MoKα radiation ($\lambda = 0.71073$ Å) at 293 K. Empirical absorption correction (Ψ scan) was applied. The structures were solved by the direct method and refined by the Full-matrix least-squares on F^2 using the SHELXL-97 software [13]. All of the non-hydrogen atoms were refined anisotropically. **1** and **2** crystallize in the space Cc and $Pna2_1$ as determined by the systematic absence in the intensity data, and successful solution and refinement of the structures, the final structural Flack parameter $K = 0.00$, suggesting the absolute configuration of the compounds can be confirmed. The hydrogen atoms were located from difference Fourier maps. The crystal data and structure refinement of compounds **1** and **2** are summarized in Table 1. The selected bond lengths and angles of compounds **1** and **2** are listed in Table 2.

3. Results and discussions

3.1. Synthesis

We first carried out the experiments in mild and classical synthesis conditions, unfortunately, the expected single crystals could not obtained. Recently, plentiful practices have proved that hydrothermal method is very effective for the synthesis of coordination polymers. Consequently, we adopted hydrothermal method. The isolation of **1** depended vitally on the reaction pH value. Better crystals and single phase only can be obtained at pH 4.5. If the reaction was performed at pH 3.5–4.5 or 4.5–5.5, we could not obtain better crystals but only polycrystals. If the reaction was performed at other pH value, a lot of green precipitate was given.

3.2. Description of the structures

$[Ni(H_2O)(C_4H_4O_5)] \cdot H_2O$ **1**: The single-crystal X-ray analysis reveals that compound **1** exhibits a 3D framework with multidirectional 1D channels. The asymmetric unit contains one independent Ni atom, which is octahedrally coordinated by one aqua ligand and five oxygen atoms with four from three separated malate groups and one hydroxyl oxygen atom. The Ni–O bond lengths range from 2.034(5) to 2.101(5) Å, as shown in Fig. 1. All malate ligands are equivalent, although D-, L-type malate groups play different structural roles. Each malate group acts simultaneously as a tridentate (O1, O3, O4) and bis-monodentate (O2, O5) coordination modes bridging three Ni ions. The valence sum calculation gives the value of 1.2 for the α-hydroxy oxygen, indicating that it is a protonated oxygen atom.

Interesting, D-, L-type malate ligands are alternatively arranged linking Ni atoms to generate a 2D sheet (Fig. S1). Adjacent layers are covalently linked by the remaining β-carboxylic groups of D-type malate groups as molecular pillars to form a 3D framework. A remarkable feature is the presence of pores running along [101] direction and c-axis. The 3D network

Table 1
Crystal data and structure refinement for compounds **1** and **2**

Empirical formula	$C_4H_8NiO_7$	$C_{16}H_{14}N_2NiO_6$
Formula weight	226.81	389.00
Temperature (K)	293(2)	293(2)
Crystal system	Monoclinic	Orthorhombic
Space group	*Cc*	*Pna*2(1)
a (Å)	13.156(3)	9.6113(2)
b (Å)	7.5436(2)	19.691(4)
c (Å)	9.6982(2)	8.0944(2)
α (°)	90	90
β (°)	130.96(3)	90
γ (°)	90	90
Volume (Å³)	726.8(2)	1531.9(5)
Z	4	4
D_c (g cm^{-3})	2.073	1.687
μ (mm^{-1})	2.668	1.305
F (000)	464	800
Crystal size (mm)	$0.530 \times 0.320 \times 0.150$	$0.120 \times 0.140 \times 0.100$
GOF	1.083	0.744
Final *R* indices [$I > 2\sigma(I)$]	$R_1 = 0.0599^a$, w$R_2 = 0.1673^b$	$R_1 = 0.0382^a$, w$R_2 = 0.0701^b$
Indices (all data)	$R_1 = 0.0613^a$, w$R_2 = 0.1690^b$	$R_1 = 0.0551^a$, w$R_2 = 0.0762^b$

[a] $R_1 = \sum ||F_o| - |F_c|| / \sum |F_o|$.
[b] w$R_2 = \{\sum[w(F_o^2 - F_c^2)^2] / \sum[w(F_o^2)^2]\}^{1/2}$.

Table 2
Selected bond lengths (Å) and angles (°) for compounds **1** and **2**

1

Ni(1)–O(2)#2	2.036(5)	Ni(1)–O(5)#1	2.034(5)
Ni(1)–O(3)	2.061(5)	Ni(1)–O(1W)	2.071(5)
Ni(1)–O(1)	2.073(5)	Ni(1)–O(4)	2.101(5)
O(5)#1–Ni(1)–O(2)#2	90.6(2)	O(2)#2–Ni(1)–O(3)	95.1(2)
O(5)#1–Ni(1)–O(3)	169.4(2)	O(2)#2–Ni(1)–O(1W)	92.3(2)
O(5)#1–Ni(1)–O(1W)	95.0(2)	O(3)–Ni(1)–O(1W)	93.7(2)
O(2)#2–Ni(1)–O(1)	174.4(2)	O(1W)–Ni(1)–O(1)	92.0(2)
O(3)–Ni(1)–O(1)	81.1(2)	O(5)#1–Ni(1)–O(4)	89.2(2)

2

Ni(1)–O(1)	2.032(3)	Ni(1)–OW1	2.026(4)
Ni(1)–O(3)	2.048(3)	Ni(1)–O(2)	2.111(3)
Ni(1)–N(2)	2.060(3)	Ni(1)–N(1)	2.099(3)
OW1–H(1A)	0.869(2)	OW1–H(1B)	0.85(2)
OW1⋯O1	2.619	OW1–H(1A)⋯O1	2.619
O2–H(2)⋯O5	2.677		
O(1)–Ni(1)–OW1	95.75(2)	O(1)–Ni(1)–O(3)	94.78(13)
OW1–Ni(1)–O(3)	88.38(14)	O(1)–Ni(1)–N(2)	166.01(2)
OW1–Ni(1)–N(2)	92.21(2)	O(1)–Ni(1)–N(1)	92.87(12)
N(2)–Ni(1)–N(1)	79.22(12)	O(1)–Ni(1)–O(2)	78.75(12)
OW1–H(1A)⋯O1	145.54	O2–H(2)⋯O5	174.24

Symmetry transformations used to generate equivalent atoms: #1: *x*, $-y+1$, $z-1/2$, #2: $x-1/2$, $-y+3/2$, $z-1/2$.

Fig. 1. The coordination environments of nickel atom in compound **1**. Hydrogen atoms are omitted for clarity.

consists of pentagonal channels running along the [101] direction with dimensions 5.243×5.318 Å (based on $d_{\text{Ni} \cdots \text{Ni}}$) (Fig. 2). The coordinated water molecules point at the channels and non-coordinated water molecules located in the channels. Trapezoidal channels down *c*-axis possess approximate dimensions of 7.583×7.583 Å and w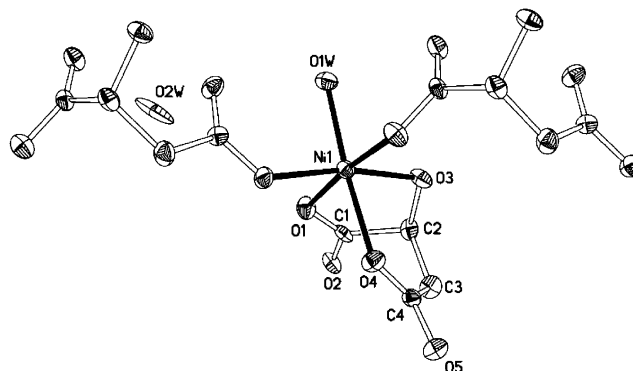ere occupied by non-coordinated water molecules, involving hydrogen bonds between the carboxyl oxygen atoms and coordinated water molecules, which further consolidated the stability of the framework (Fig. 3, Fig. S2). Each cavity at the intersection of the perpendicular tunnels contains one independent water molecule.

The structure can be described as a covalently bonded diamond-like network, if the Ni atoms are regarded as four-connecting nodes (Fig. 4). Although coordination polymers with diamond-like structure have been reported before, most of them present different degrees of interpenetration in their diamond-like arrays, and few examples show a non-interpenetrating diamond-like framework [7b,14,15]. The steric effects of α-hydroxy groups might play a crucial role in forming the non-interpenetrating diamond-like structure of compound **1**.

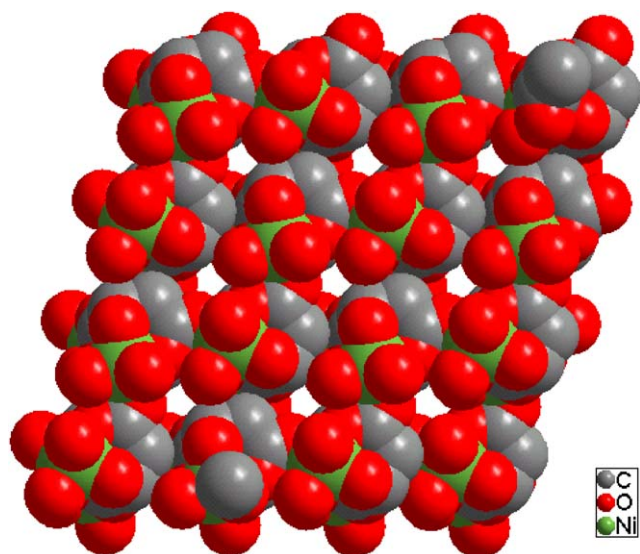Fig. 2. Space-filling diagram of complex **1** viewed along [101] direction. Hydrogen atoms are omitted for clarity.
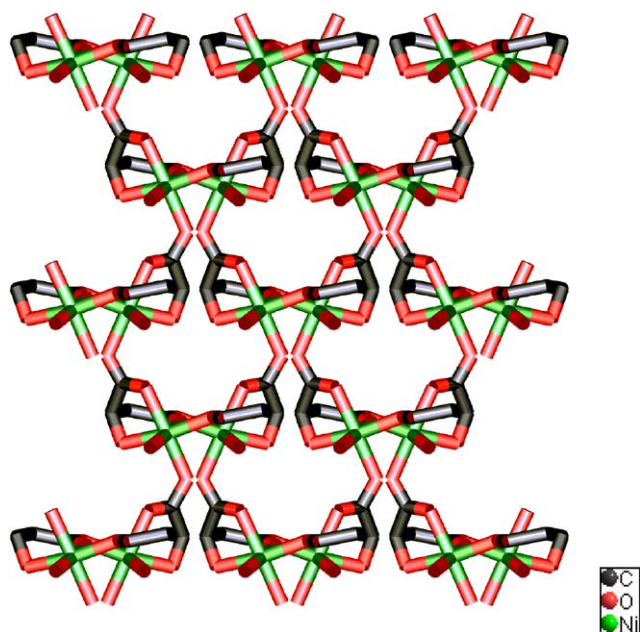

Fig. 4. Projection of **1** showing the non-interpenetrating diamond-like network based on the Ni–Ni connections.

Fig. 3. View of packing along the *c*-axis showing the trapezoidal channels (Ni = green, O = red, C = gray). Hydrogen atoms are omitted for clarity.

Fig. 5. (a) The coordination environments of nickel atom in compound **2**. Hydrogen atoms are omitted for clarity. (b) View of the hydrogen-bonded 2D supramolecular assembly of compound **2**. Hydrogen atoms are omitted for clarity.

To our knowledge, compound **1** represents the first example of a metal-organic complex having diamond-like network in the system of hydroxycarboxylic acid.

[Ni(H$_2$O)(mal)(phen)] **2**: The single-crystal X-ray analysis reveals that compound **2** exhibits a 3D supramolecular framework constructed from infinite spiral-shaped coordination polymeric chains. The fundamental unit of **2** is shown in Fig. 5a. There is one crystallographically unique Ni center in the crystal
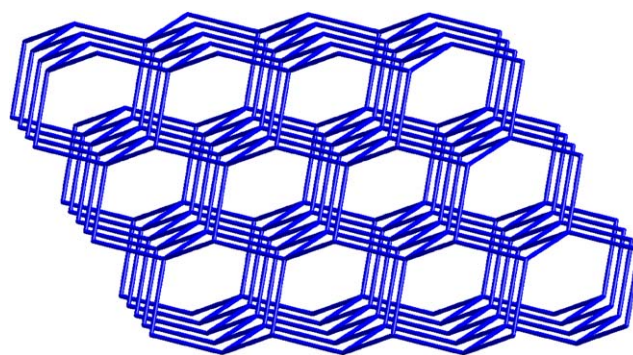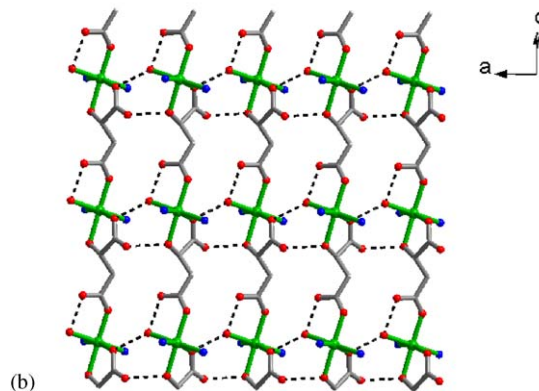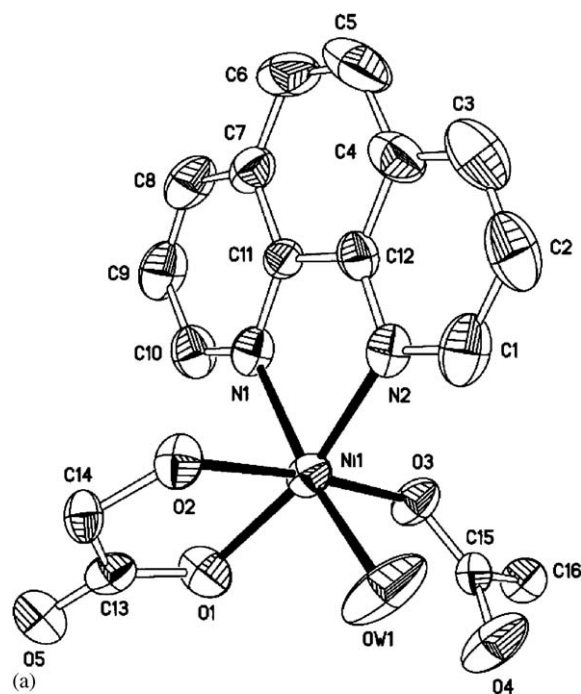
structure. The Ni center, which is in a distorted octahedral coordination geometry, coordinated to one aqua ligand, two nitrogen atoms of one 1,10′-phen group, and three oxygen atoms with two from two separated malate groups and one hydroxyl oxygen atom. The Ni–N bond lengths vary from 2.060(3) to 2.099(3) Å, and the Ni–O bond lengths are in the range of 2.026(4)—2.111(3) Å. Each malate group acts as a bidentate–monodentate ligand bridging two Ni ions. The valence sum calculation gives the value of 1.17 for the α-hydroxy oxygen atom, indicating that it is a protonated oxygen atom. The non-linear flexible malate ligands connect two Ni atoms to form spiral-shaped chains with the phen ligands arranged uniquely at one side of the chains. There are persistent O–H···O hydrogen bond interactions between the chains (Fig. 5b) with O···O distances in the range of 2.619–2.677 Å indicating the existence of strong O–H···O hydrogen bonds. It is found that the coordination fashions of malate groups and the 2D sheets formed via hydrogen bonds in both **2** and **L** are greatly similar. However, the overall crystal structure of **2** is different from the porous supramolecular architecture of **L**, which may stem from the difference of organonitrogen ligands. The phenanthroline ligand, possessing larger volume than 2,2′-bpy, insert the void space formed within the supramolecular framework, and dramatically influence the final structure [16].

3.3. Characterization

Variable-temperature magnetic behavior of **1** is displayed in Fig. 6. The value of the magnetic moment at room is $3.13\,\mu_{\rm B}$ per nickel ion. Upon lowering the temperature, $\mu_{\rm eff}$ gradually increases from 3.13 at 300 K to $4.85\,\mu_{\rm B}$ at 4 K, showing a ferromagnetic interaction. However, the curve rapidly decreases below 4 K, indicating that a much weaker antiferromagnetic inter-
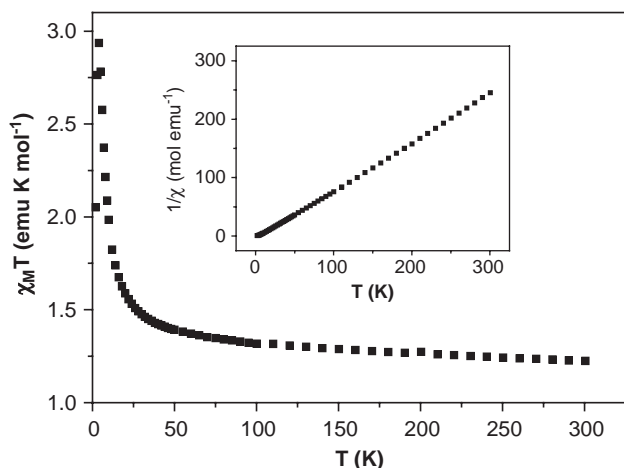
action exists in **1** at low temperatures. The inverse susceptibility plot as a function of temperature is linear, closely following the Cure–Weiss law with $C = 1.22\,{\rm emu\,K\,mol^{-1}}$, corresponding to about one $S = 1$ spin per formula unit with $g = 2.21$ for Ni(II) centers. The Weiss temperature $\theta = 1.913\,{\rm K}$, indicating that there exist predominantly ferromagnetic interactions in **1**. According to the crystal structure of **1**, it can be assumed that the magnetic behavior of **1** may be due to the superexchange interactions between Ni(1) and Ni(1 g) centers through the carboxylato bridges.

The IR spectrum of compound **1** (Fig. S3a) shows strong band of carboxyl group at $1539\,{\rm cm^{-1}}$ for the antisymmetric stretching and at 1435, 1400, 1354, $1292\,{\rm cm^{-1}}$ for symmetric stretching. The separations (Δ) between $v_{\rm asym}$ (OCO) and $v_{\rm sym}$ (OCO) indicate that the malate ligands coordinate to the metal in both monodentate and multidentate fashions [17], which is consistent with the crystal structure of **1**. The stretching band in 3422, $3509\,{\rm cm^{-1}}$ is characteristic of $v_{\rm O-H}$. The IR spectrum of **2** is shown in Fig. S3b. The separations (Δ) between $v_{\rm asym}$ (OCO) and $v_{\rm sym}$ (OCO) indicate that the malate ligand is monodentate and bidentate coordination mode in compound **2** [17], which is consistent with the crystal structure of **2**.

The TG curve of compound **1** (Fig. S4a) exhibits two continuous weight loss stages. The first weight loss is 16.15% in the temperature range 140–275 °C, corresponding to the loss of water molecular and aqua ligand. The remaining two weight losses are 51.22% in the temperature range of 275–380 °C, corresponding to the removal of coordinated malate ligands. The whole weight loss (ca. 67.37%) is in good agreement with the calculated value (67.07%). The sample does not lose weight at temperatures higher than 380 °C. The TG curve of compound **2** (Fig. S4b) exhibits two weight loss steps. The first weight loss starts at ca. 170–230 °C to give a total weight loss of 4.42%, corresponding to the loss of coordinated water molecular (4.63%). The second weight loss starts at ca. 320–420 °C (76.40%), corresponding to the removal of coordinated malate and phen ligands.

4. Conclusion

In conclusion, we have successfully designed and prepared two nickel coordination complexes. Compound **1** shows a 3D open framework with two types of cavities by means of flexible saturated hydroxycarboxylic acid as ligand. Compound **2** displays a 3D supramolecular framework based on 1D spiral-shaped chains. This work implies that new structures with unique structural features may be isolated in metal–malic acid system by varying the synthetic conditions.

Fig. 6. Thermal variation of $\chi_{\rm m}T$ and $1/\chi_{\rm m}$ for compound **1**.

5. Supplementary materials

Crystallographic data for the structural analysis have been deposited with the Cambridge Crystallographic Data Center, CCDC-249996 and 253116. These data can be obtained free of charge on application to CCDC, 12, Union Road, Cambridge CB2 1EZ, UK (Fax: +44-1223/336-033; E-mail: deposit@ccdc.cam.ac.uk).

Acknowledgments

Appendix A. Supplementary materials

The online version of this article contains additional supplementary data. Please visit doi:10.1016/j.jssc.2004.12.042.

References

[1] B. Moulton, M.J. Zaworotko, Chem. Rev. 101 (2001) 1629.

[2] O.M. Yaghi, H.L. Li, C. Davis, D. Richardson, T.L. Groy, Acc. Chem. Res. 31 (1998) 474.

[3] H.L. Li, M. Eddaoudi, M. O'Keeffe, O.M. Yaghi, Nature 402 (1999) 276.

[4] (a) M. Eddaoudi, D.B. Moler, H.L. Li, B.L. Chen, T.M. Reineke, M. O'Keeffe, O.M. Yaghi, Acc. Chem. Res. 34 (2001) 319;
(b) S. -I. Noro, S. Kitagawa, M. Kondo, K. Seki, Angew. Chem. Int. Ed. 39 (2000) 2081.

[5] (a) X.H. Bu, M.L. Tong, H. –C. Chang, S. Kitagawa, S.R. Batten, Angew. Chem. Int. Ed. 43 (2004) 192;
(b) K. Biradha, Y. Hongo, M. Fujita, Angew. Chem. Int. Ed. 39 (2000) 3843.

[6] L.S. Long, X.M. Chen, M.L. Tong, Z.G. Sun, Y.P. Ren, R.B. Huang, L.S. Zheng, J. Chem. Soc., Dalton Trans. (2001) 2888.

[7] (a) E.W. Lee, Y.J. Kim, D.Y. Jung, Inorg. Chem. 41 (2002) 501;
(b) T.F. Liu, H.L. Sun, S. Gao, S.W. Zhang, T.C. Lau, Inorg. Chem. 42 (2003) 4792.

[8] (a) R. Vaidhyanathan, S. Natarajan, C.N.R. Rao, Solid State Sci. 4 (2002) 633;
(b) R. Vaidhyanathan, S. Natarajan, C.N.R. Rao, J. Chem. Soc., Dalton Trans. (2003) 1459.

[9] (a) C. Livage, C. Egger, G. Férey, Chem. Mater. 11 (1999) 1546;
(b) N. Guillou, C. Livage, W. van Beek, M. Noguès, G. Férey, Angew. Chem. Int. Ed. 42 (2003) 643.

[10] (a) Z.H. Zhou, S.Y. Hou, H.L. Wan, J. Chem. Soc., Dalton Trans. (2004) 1393;
(b) J.J. Cruywagen, L. Krüger, E.A. Rohwer, J. Chem. Soc., Dalton Trans. (1997) 1925.

[11] (a) Z.H. Zhou, G.F. Wang, S.Y. Hou, H.L. Wan, K.R. Tsai, Inorg. Chim. Acta (2001) 184;
(b) X.L. Liu, X.H. Liu, J.J. Yue, Y.X. Yin, Y. Sun, J. Mol. Struct. (2004) 87.

[12] Y.Q. Guo, H.Y. An, Y.G. Li, E.B. Wang, X.L. Wang, L. Xu, C.W. Hu, Inorg. Chim. Acta (2004) 4582.

[13] (a) G.M. Sheldrick, SHELXL 97, Program for Crystal Structure Refinement, University of Gőttingen, Germany, 1997;
(b) G.M. Sheldrick, SHELXL 97, Program for Crystal Structure Solution, University of Gőttingen, Germany, 1997.

[14] (a) E. Siebel, A.M.A. Ibrahim, R.D. Fischer, Inorg. Chem. 38 (1999) 2530;
(b) S. Lopez, M. Kahraman, M. Harmata, S.W. Keller, Inorg. Chem. 36 (1997) 6138;
(c) T. Kuroda-Sowa, T. Horino, M. Yamamoto, Y. Ohno, M. Maekawa, M. MunaKata, Inorg. Chem. 36 (1997) 6382.

[15] (a) S.J. Retting, V. Sánchez, A. Storr, R.C. Thompson, J. Trotter, J. Chem. Soc., Dalton Trans. (2000) 3931;
(b) B.F. Hoskins, R. Robson, J. Am. Chem. Soc. (1990) 1546.

[16] (a) X.M. Chen, G.F. Liu, Chem. Eur. J. 8 (2002) 4811;
(b) Y.Z. Zheng, G.F. Liu, B.H. Ye, X.M. Chen, Z. Anorg. Allg. Chem. 630 (2004) 296.

[17] K. Nakamoto, Infrared and Raman Spectra of Inorganic and Coordination Compound, fifth ed, Willey, New York, 1997.